Gradient approach to INSAR modelling of glacial dynamics and morphology

A. I. Sharov
Institute of Digital Image Processing, Joanneum Research, Wastiangasse 6, A - 8010 Graz, Austria
E-mail: aleksey.sharov@joanneum.at

Keywords: differential interferometry, phase gradient, change detection, glacier velocity, geodetic survey

ABSTRACT: This paper describes the development and testing of an original gradient approach (GINSAR) to the reconstruction of glacial morphology and ice motion estimation from the interferometric phase gradient that does not involve the procedure of interferometric phase unwrapping, thus excluding areal error propagation and improving the modelling accuracy. The global and stringent GINSAR algorithm is applicable to unsupervised glacier change detection, ice motion estimation and glacier mass balance measurement at regional scale. Experimental studies and field surveys proved its efficacy and robustness. Some algorithmic singularities and limitations are discussed.

1 INTRODUCTION

There is a close interrelation between glacier motion and glacial topography. Irregularities in the glacier width, thickness, slope or direction alter the character of ice flow. On the other hand, glacial topography is dynamically supported by the moving ice (Fatland & Lingle 1998). Both, glacier dynamic quantities and topographic variables are essential parameters for studying the glacier mass balance and monitoring actual and potential glacier changes. The detailed and equivalent spatial models derived from remote sensing data that reliably describe the glacier shape and spatial distribution of ice velocity at different instants of time are of fundamental significance for such studies.

While the generation of glacier surface models, e.g. by stereophotogrammetric methods, is well established, the generation of glacier kinematic models representing the ice flow pattern or velocity vector field still remains an area of active research. This is mostly because of the typically low velocity of glacier ice motion that restricts the application of remote sensing data with limited spatial resolution and short temporal coverage. The common rate of flow of the Alpine glaciers is from ten to twenty inches per day in summer, and about half that in winter (Webster's Revised Unabridged Dictionary, 1998). The ground resolution of available remote sensing data is somewhat coarser and a quite long time interval (months to years) between subsequent surveys is usually required in order to detect and to measure the glacier motion accurately.

The advancement of satellite radar interferometry (INSAR) in the 1990s gave new impetus to the study of glacier dynamics from space. Apart from large terrestrial coverage of up to 10,000 km² and general advantages of all-weather SAR systems, the INSAR method provides an astonishing opportunity to detect and to measure quite small glacier motions and ice deformations in the centimetre range from spaceborne SAR interferograms with a nominal ground resolution of several tens of meters. Accurate reconstruction of the configuration and external structure of the glacier surface from INSAR data is also possible. Differential interferometry (DINSAR) based on differencing between two different SAR interferograms of the same glacier allows the impacts of glacial topography and surface displacement on the interferometric phase to be analysed separately, but involves some technological complications and restrictions (Gabriel et al. 1993).

This paper reports on the design of a stringent, albeit very simple algorithm for the reconstruction of glacial morphology and ice motion estimation from the interferometric phase gradient that does not involve complex process artifices and does not require additional topographic reference models. The following methodical sequence of actions is considered

- calculation of interferometric phase gradients and their conversion to the glacier slope map;
- unsupervised glacier change detection by differencing multitemporal INSAR slope maps;
- determination of glacier dynamic quantities and estimation of mass balance components such as longitudinal strain rate, motion field, flux divergence, etc.;
- verification of results by field surveys in the European Arctic.

An experimental data set included the ERS-1/2-INSAR pairs obtained over the Svartisen Ice Cap in Norway and the Northern Ice Dome in Novaya Zemlya, Russia, which were processed using the RSG 4.1 software package. Terrestrial surveys of glacier velocities were undertaken at 5 outlet glaciers in Novaya Zemlya in September 2001.

2 INSAR MODELLING OF THE GLACIER SURFACE: SLOPE MAP VERSUS DEM

In addition to glaciological maps, two basic types of spatial models are presently used for the documentary representation of the glacier surface:

- *topographic models* represent the glacier relief by specifying the geodetic location and absolute elevation of glacier points with respect to the standard reference surface or co-ordinate system;
- *morphometric models* describe quantitatively the configuration and external structure of the glacier surface by specifying relative spatial parameters.

A digital elevation model (DEM) and a slope map/model (SM) are typical examples of topographic and morphometric models, respectively. In common practice, slope maps are produced as a secondary product from available DEMs by using standard algorithms. An inverse procedure is seldom performed.

At the 21st EARSeL Symposium in Paris it was demonstrated, however, that the direct production of glacier slope maps from INSAR data could be performed in a more straightforward and a much less complicated manner than by interferometric DEM generation. An original gradient approach to geometric processing of SAR interferometric data (GINSAR) has been shown to be capable of providing quite accurate glacier slope maps (Sharov et al. 2002). The underlying concept of the GINSAR technique is based on the transition from performing operations on original SAR interferograms to the analysis of their derivatives. Differentiation of original interferometric phase results in the gradient picture, which provides a realistic view of the terrain and can be unambiguously related to the glacier relief (Fig. 1, a, b, c, d).

The partial derivatives of interferometric phase $\varphi(x,y)$ in azimuth (x) and in range (y) direction are well approximated by differences as (Sharov & Gutjahr 2002)

$$\frac{\partial\varphi(x,y)}{\partial x} \cong \nabla\varphi_x(x,y) = \frac{\varphi(x+\Delta x,y)-\varphi(x,y)}{\Delta x} \quad \text{and}$$
$$\frac{\partial\varphi(x,y)}{\partial y} \cong \nabla\varphi_y(x,y) = \frac{\varphi(x,y+\Delta y)-\varphi(x,y)}{\Delta y}. \qquad (1)$$

Thus, in our practice, the phase derivatives are calculated by subtracting an original interferential picture from a translated version of the same interferogram. In mathematics, such an approach to image differentiation is known as *method of finite differences* (Piskunov 1978). The shift values Δx and Δy are equal 1 pixel usually, but, in general, can be manipulated separately in azimuth and range direction within the interval from 0 to several pixels. The next relation gives another useful approximation using the *central difference*

$$\frac{\partial\varphi(x,y)}{\partial x} \cong \frac{\varphi(x+\Delta x,y)-\varphi(x-\Delta x,y)}{2\Delta x} \quad \text{and}$$
$$\frac{\partial\varphi(x,y)}{\partial y} \cong \frac{\varphi(x,y+\Delta y)-\varphi(x,y-\Delta y)}{2\Delta y}. \qquad (2)$$

Further increase in the shift value coarsens the spatial resolution of the topogram.

The full two-dimensional derivative of interferometric phase is given as an algebraic sum of partial derivatives

$$d\varphi(x,y) = \frac{\partial\varphi(x,y)}{\partial x}dx + \frac{\partial\varphi(x,y)}{\partial y}dy \cong \nabla\varphi_x\cdot\Delta x + \nabla\varphi_y\cdot\Delta y$$
$$\text{or} \quad \nabla\varphi(x,y) = \varphi(x+\Delta x,y) + \varphi(x,y+\Delta y) - 2\varphi(x,y). \qquad (3)$$

The value of the phase derivative is proportional to the difference in grey level between adjacent pixels of the interferogram and can take both positive and negative values.

The biggest advantage of such an approach to INSAR data processing is probably that the resultant picture can be scaled with any real, not necessarily integer factor, that makes further processing flexible and allows for any linear combination between the derivatives obtained from different interferograms. Considering the discrete character of the interferometric phase, partial derivatives $\nabla\varphi_x$ and $\nabla\varphi_y$ can be directly converted to the relative height increments Δh_x and Δh_y by using the next equation

$$\Delta h_{x,y} \cong C(x,y)\cdot\nabla\varphi_{x,y}, \qquad (4)$$

where $C(x,y) = 0.25\pi^{-1}\cdot\lambda\cdot B_\perp^{-1}(x)\cdot R(y)\cdot\sin\theta(y)$ (5)

is the conversion factor depending on the imaging geometry; λ = 5.66 cm is the wavelength of SAR signal, $B_\perp(x)$ is the length of the perpendicular component of spatial baseline, $R(y)$ - the slant range, $\theta(y)$ - the look angle.

The full height increment is defined as follows

$$\Delta h(x,y) \cong C(x,y)\cdot\nabla\varphi(x,y) = \Delta h_x\cdot\Delta x + \Delta h_y\cdot\Delta y. \qquad (6)$$

The INSAR image product specifying continuously the glacier height increments is called *topogram*. Our topograms are represented in the form of an RGB image. The first two layers give the partial height increments Δh_x and Δh_y. The third layer is occupied with the full height increment representing the rate of increase of $h(x,y)$ per unit distance. One typical example of an INSAR topogram showing Fingerbreen Outlet Glacier at the Eastern Svartisen Ice Cap, Northern Norway is given in Figure 1, d.

The terrestrial slope value ε can be calculated on a pixel-by-pixel basis as follows

$$\varepsilon = \arccos\left[\Delta p \cdot \left(\Delta h_x^2 + \Delta h_y^2 + \Delta p^2\right)^{-0.5}\right], \qquad (7)$$

where Δp is the pixel diagonal size on the ground depending on the kind of product, e.g. $\Delta p \approx 28\ m$ in 5-look ERS-1/2-SAR interferometric products and, in 20-look interferograms, we have $\Delta p \approx 56\ m$. The formula (7) provides a basic equation for transforming the INSAR topogram in the slope map.

INSAR slope maps are also generated in the form of 3-layer images. The first two layers represent the slope values in azimuth and range direction defined separately from the next equations

$$\varepsilon_x = \tan^{-1}\left(\Delta h_x / \Delta p_x\right) \quad \text{and} \quad \varepsilon_y = \tan^{-1}\left(\Delta h_y / \Delta p_y\right), \qquad (8)$$

where $\Delta p_x \approx \Delta p_y$ is the pixel size on the ground.

The third layer shows the absolute slope value ε. In special applications, the conversion factor $F(x,y)$ can be presented as an additional fourth layer to the slope map or topogram. An example of an INSAR slope map is given in Figure 2, b.

Visual inspection of coloured slope maps showed that the spatial resolution of original interferograms was nearly preserved and about 75% of fine details on the glacier surface were still detectable. Different slope maps of the same terrain looked very similar in spite of the fact that they were generated from INSAR data originating from different seasons and having different geometry, e.g. the relative shift in terrestrial coverage of 70 kilometres. This fact indicates, at least qualitatively, the correctness of surface modelling.

The metric quality of our INSAR slope maps was evaluated by comparing them with the reference slope map obtained from the large-scale DEM. Tests performed by several independent experts have verified good modelling accuracy with the mean slope difference between 3 models of less than 0.1°. The rms slope difference was given as 0.51° for steady slopes of less than 23° (SAR look angle). Slope values were quite tolerant of local phase errors and the GINSAR algorithm remained feasible even under significant phase noise.

The INSAR SMs provide valuable information on the possible character of glacial flow and incident sun radiation, though they cannot be directly used for determining glacier elevations. Nevertheless, any glacier SM can be transformed into a glacier DEM by integrating height increments $\Delta h(x, y)$.

Gradient approach to INSAR glacier modelling based on simple deterministic procedures ensures serious processional advantages. The procedure of GINSAR SM generation involves less complicated operations than that of producing the INSAR DEM, yet without compromising on accuracy. All technological operations involved act globally, i.e. over the whole image scene without gaps. For the great majority of points in the interferential picture partial derivatives of the wrapped phase are equal to partial derivatives of the unwrapped phase. Therefore, the interferometric phase unwrapping, which is reputed to be the most sophisticated and problematic calculus in interferometric signal processing, becomes redundant, thus excluding areal error propagation and the necessity for phase filtering. The computational load is thus essentially reduced. The production of GINSAR SMs is to be preferred in particular in the case of a lack of reliable ground control data and reference models, which are typical situations in glacial areas.

Another significant advantage of the GINSAR technique can be recognised at the stage of differential INSAR data processing aimed at glacier change detection and motion estimation. At all events it is worth quoting Prof. M. Kuhn from Innsbruck University who said that DEMs are used more frequently than slope maps in glaciology, *"...mostly because of the common trade"* (personal communication 2001).

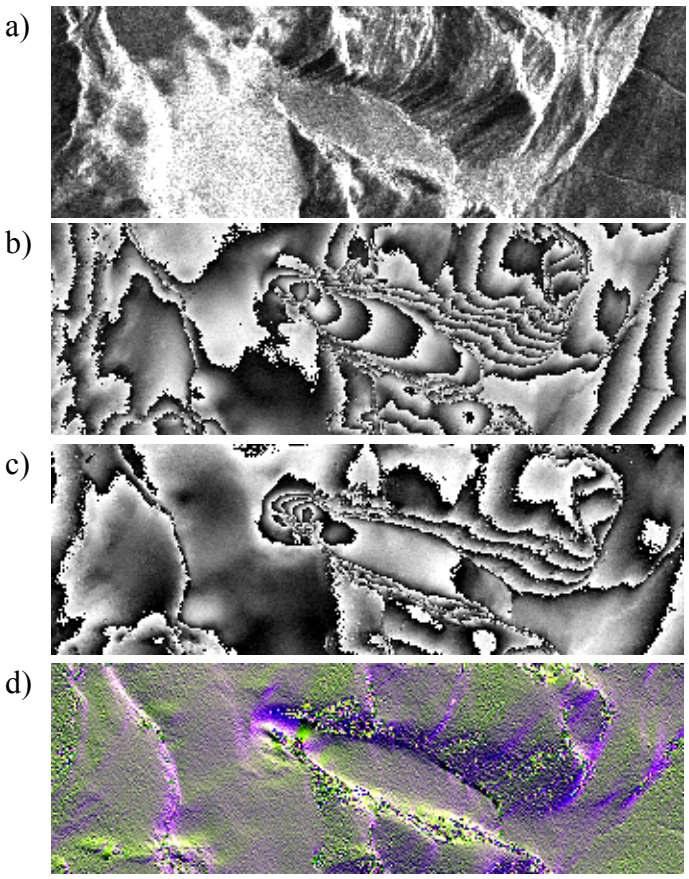

Figure 1. INSAR products of Fingerbreen Glacier, North. Norway: amplitude image (a), fringe image of 16/17.03.96 (b) and 01/02.04.96 (c), topogram (d).

3 HOW TO SEPARATE GLACIER MOTION FROM TOPOGRAPHY

Movement is an inherent quality of any active glacier, and the Greek phrase *panta rhei*, i.e. *all things are in flux*, provides an adequate formula expressing the basic feature of a typical glacier environment. In a traditional stereophotogrammetric model or a single-pass SAR interferogram, if alone, the glacier motion cannot be registered because of the very short time interval between takes of images constituting a stereo or INSAR pair. In repeat-pass SAR interferograms, phase contributions by both glacial flow and topography are recorded and mixed together. It is virtually impossible in practical terms to find out the real repeat-pass INSAR model of a living glacier without topographic and motion fringes.

In general, the INSAR scheme is much more sensitive to the surface motion than to the surface relief, and the rate of motion fringes in the interferential picture of a polar valley glacier is usually much higher than that of topographic fringes. Under the relatively flat topography of ice caps and rather high velocities of ice flow in outlet glaciers, the differentiation procedure emphasises the motion component and partly or completely attenuates the topographic one. The local qualitative analysis of ice motion can, therefore, be performed even in single topograms. A full separation between the impacts of glacier topography and glacier motion on the interferometric phase remains necessary for the highly accurate detection and measurement of glacier dynamics.

If the glacier topography is assumed to be unchanged between the instants of multitemporal INSAR surveys, its contribution to the interferometric phase can be excluded by differencing between two co-registered multitemporal INSAR topograms or slope maps of the same glacier. Third layers in topograms and slope maps can be compared with the corresponding products obtained from other interferograms more or less independently of their range and azimuth direction. Assuming that $\nabla\varphi = \nabla\varphi_{topo} + \nabla\varphi_{mot}$ and $C_1 \cdot \nabla\varphi_{topo\,1} = C_2 \cdot \nabla\varphi_{topo\,2}$, the operation of differencing between the third layers of two topograms can be formulated as follows

$$F = C_1 \cdot \nabla\varphi_{mot\,1} - C_2 \cdot \nabla\varphi_{mot\,2}. \quad (9)$$

The resultant picture *F(x,y)* containing only the differential motion phase without topographic phase is called *fluxogram* following the definition given by I. Newton to differential calculus (*fluxions*, from Latin flüxus – flow, continual change). The fluxogram is represented in the form of a 4-layer image with the first two layers showing the difference between scaled partial motion increments in azimuth and range direction. The third layer shows the difference between full motion increments and the fourth layer gives the direction of differential motion calculated as the ratio between the first two layers.

An example showing a small fragment from the fluxogram generated from two INSAR data sets obtained over the Svartisen Ice Cap in Northern Norway on 16/17 March and 1/2 April 1996 is presented in Fig. 2, c). A topogram of the same area is given in Fig. 2, a) for the purpose of comparison. One can see that, in the fluxogram, objects undergoing temporal changes can be clearly distinguished from those that did not change between INSAR surveys. Therefore, such a product is sometimes called a *change image*. Different tracts of the glacial area are shown in brown, yellow or blue colour depending on the change direction. The steady rocky areas surrounding the ice cap are represented in a uniform shade of silver and appear completely "flat". Inland borders of the ice cap and especially those of outlet glaciers can be reliably delineated. The areas of speckle noise correspond to localities with incoherent character of changes / flow.

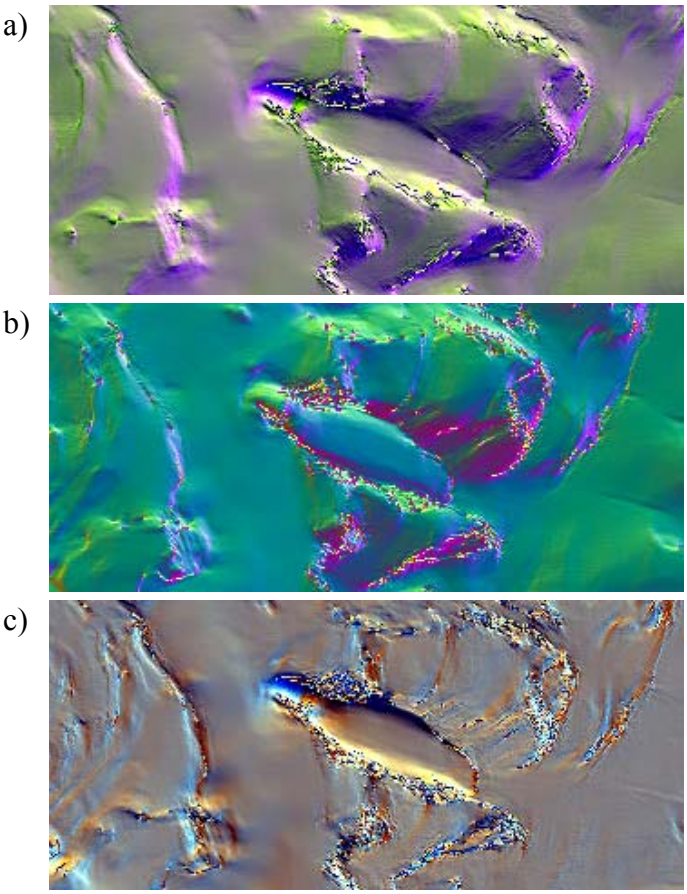

Figure 2. Topogram (a), slope map (b) and fluxogram (c) of Fingerbreen Glacier, Est. Svartisen

A very interesting fact is that, in the fluxogram, glacier changes can be observed over the whole area of the ice cap, even in its upper parts and the ice cap appears to be standing out among non-glaciated rocky surroundings that seem to be quite level. This effect cannot be explained by the influence of radar penetration in the dry snow because the entire glacier surroundings were also covered with snow during the period of the INSAR surveys, but there are no significant changes to be observed in the ice-free terrain. Besides this, the relative amount of the glacier changes decreases continuously upwards.

The only reasonable explanation for this effect is that, in a steady-state glacier maintaining its profile or surface, the surplus of snow/ice deposited in the accumulation area has to be transported to the ablation zone, and there is a motion over the entire glacier area even in the cold season. The motion is mainly vertical at the top of the glacier and is surface parallel near the glacier border/snout. Assuming 300 cm accumulation a year over the Svartisen Ice Cap (Kjöllmoen 2002) one can obtain a vertical velocity of nearly 1 cm/day at the glacier top, corresponding to about one third of a motion fringe. In outlets, the ice velocity is naturally much higher.

In this context, it is worth noting that the preliminary interpretation of the fluxogram has been performed practically without ground-truth data, which is why we can refer to unsupervised glacier change detection. Nevertheless, this finding argues that even slight changes in the character of vertical motion at the glacier top can be detected and temporal variations of the accumulation rate can be derived from the fluxogram at the regional scale.

4 DETERMINATION OF GLACIER DYNAMIC QUANTITIES

The direct measurement of the glacier motion from the fluxogram is still impossible because only the difference between two scaled motion phases is given. Nevertheless, the relation between the terms $C_1 \cdot \nabla\varphi_{mot\,1}$ and $C_2 \cdot \nabla\varphi_{mot\,2}$ in the equation (9) can be estimated a priori by comparing the spatial baselines and environmental conditions during the INSAR surveys. If one of these terms is much larger than the other, the fluxogram can be used directly for the quantitative estimation of the dominating motion term. Otherwise, the equation (9) can be solved, e.g. with regard to $\nabla\varphi_{mot1}$, in the following manner:

Firstly, a reference non-zero value for $\nabla\varphi_{mot2}$ has to be determined, e.g. on the basis of the transferential approach offered in (Sharov & Gutjahr 2002). Secondly, the third layer of the fluxogram is converted to a new image product using the following relation

$$\nabla\varphi_{mot\,1} = \Delta V_1 \cdot \Delta T_1 = F \cdot (C_1 - aC_2)^{-1}, \qquad (10)$$

where ΔV_1 is the velocity gradient and $\Delta T_1 = 1$ day is the spatial baseline of the first interferogram. The equation (10) is written under the assumption that the relation between the motion increments $a = \nabla\varphi_{mot\,2} / \nabla\varphi_{mot1}$ remains constant over the entire glacier area. Our experience shows that such a constraint is not always valid, especially, in glacial areas with high velocity gradients. Nevertheless, this assumption seems to be more reliable in the glacier environment than the steady flow assumption. It is interesting to note that the ratio between the conversion factors $b = C_1 / C_1$ can always be treated as a constant. According to our tests, in the majority of cases, the deviation of b from the mean value did not exceed 1 percent over the whole overlap area between two different interferograms.

Neither the fluxogram nor the topogram can be used for the direct measurement of glacial motion. These GINSAR products reproduce the value of ice-velocity gradient and provide only relative information about the glacier velocity. Nevertheless, the topogram can be directly applied to the analysis of the longitudinal glacier strain rate. The latter is usually calculated as a difference between two neighbouring velocity values divided by the distance between velocity records along the longitudinal transect (Forster et al. 1999). A graph showing the longitudinal strain rate for Fingerbreen Outlet Glacier in Eastern Svartisen Ice Cap is given in Figure 3. The initiation of crevassing recognised in topographic maps and SAR amplitude images coincides with peaks in the graph.

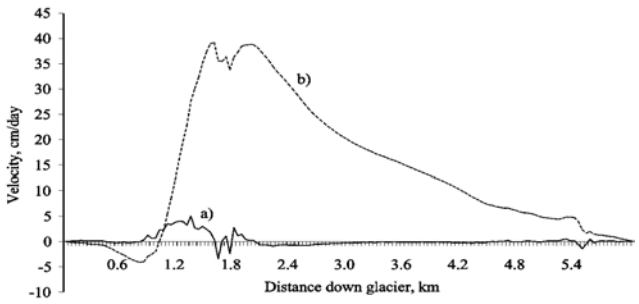

Figure 3. Fingerbreen Glacier transects of longitudinal strain rate (a) and glacier velocity (b)

In order to obtain the absolute glacier velocity, the integration of velocity gradients has yet to be performed. The results of numerical linear

integration performed in the topogram along the transect given in Fig. 3, a) are reproduced in Fig. 3, b). The maximum horizontal ice velocity in the narrow upper part of Fingerbreen Glacier attains 0.38 m/day. Figure 4 represents the *velogram* of Fingerbreen Glacier showing the spatial distribution of ice velocity over the glacier area. This velogram was obtained from the INSAR fluxogram of March-April 1996 by applying the Cholesky algorithm to solving an over-determined system of linear equations, which relate the unknown velocities with their gradual observations in a least-square manner (Sharov et al. 2002).

In Fig. 4, one can see two typical artefacts known as "bull-eyes" and, in accordance with the explanation given e.g. in (Fatland & Lingle 1998), it is supposed that their origin is related with the temporal propagation of the ice "wave" and corresponding change in the position of an ice bulge. This hypothesis seems to be in good correspondence with the quite different character of interferometric fringes in Fig. 2 b) and c) showing different dynamics in the mid part of the glacier. The lesser number of motion fringes in the interferential picture of 01/02.04.1996 indicates probably that the motion wave passed by and the glacier is in a quiescent phase again.

Another interesting approach to the integration of velocity gradients is based on the adaptation of available algorithms for one- or two-dimensional phase unwrapping. The algorithmic studies devoted to the GINSAR velocimetry are not finished yet, which is why a comprehensive description of this technique and its results in all details is not given here.

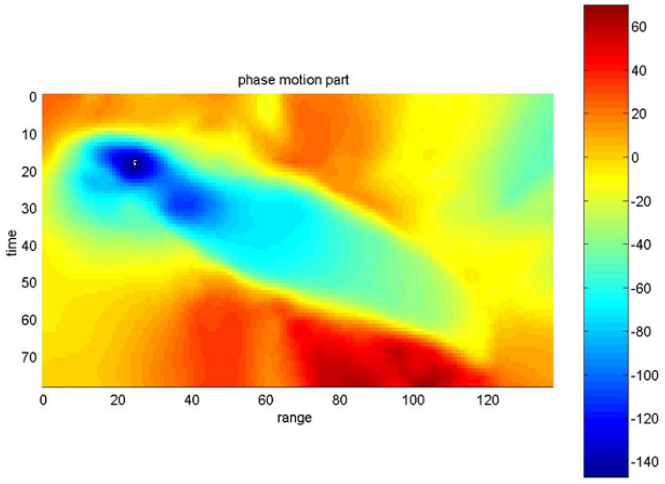

Figure 4. Velogram of Fingerbreen Outlet Glacier

The last section in Chapter 3 also provides some evidence for the applicability of the GINSAR method to the glacier mass balance measurement. Indeed, the balance of mass b per unit basal area can be defined from the next differential equation (Kuhn et al. 1999)

$$\rho \cdot \left(\frac{\partial h}{\partial t} + \frac{\partial vh}{\partial y} \right) = b \qquad \text{or}$$

$$\rho \cdot \left(\frac{\partial h}{\partial t} + \bar{h} \cdot \frac{\partial v}{\partial y} + \bar{v} \cdot \frac{\partial h}{\partial y} \right) = b\,, \qquad (11)$$

where ρ - is the ice density treated as a constant, h - is the variable thickness of the glacier, v - is the glacier longitudinal velocity measured along the distance y, and the glacier lateral flow is neglected; the bar symbol denotes spatial averaging. In equation (11), the first term in brackets represents temporal changes of the surface elevation, the second term is the ice flux divergence and the third is the advection of ice thickness.

It is believed that some, if not all, components of the specific mass balance can be measured from our INSAR products. The fluxogram is suitable for evaluating temporal changes of the surface elevation $\partial h/\partial t$. In the areas with slow (or no) motion the fluxogram can be applied to the measurement of the mean thickness of the snow/ice layer gained or lost during the balance year. Spatial gradients of the glacier velocity $\partial v/\partial y$ can be directly determined from the topogram, if the latter is obtained from the interferogram with small spatial baseline. Otherwise, the velocity gradient value is derived from the GINSAR product in accordance with the equation (10). The component $\partial h/\partial y$ can be considered as spatial changes of the surface elevation and thus can be also determined from the topogram. Averaged values of the ice thickness and glacier velocity can be calculated on the basis of available long-term data of glaciological observations.

Equation (11) shows that glacial motion and changes in the glacier surface topography are interrelated and mutually influence the glacier mass balance. Generation of an INSAR model, which could represent the spatial distribution of the product $\boldsymbol{v} \times \boldsymbol{h}$, and its subsequent differentiation as described in Chapter 2 would provide a new very promising opportunity for mass balance measurement, but has not been tried yet. In general, the INSAR system reacts on the component of surface displacement along the SAR line of sight irrespectively of the origin and kind of glacier motion/change. In order to lessen the number of variables and to simplify the measurement of mass balance from INSAR data, one can adopt that all glacier volume changes are caused solely by vertical motions. In the case that

the topographic phase is precisely compensated or vanishes, e.g. at the top of an ice cap, the relative accuracy of measuring vertical motions can be given as 5 mm, which corresponds to about one fifth of the motion fringe. Thus, the measurement of vertical motions with a magnitude of 1 cm is technically quite feasible. One should not forget, however, that the INSAR system is not sensitive to the surface displacement in the along-track direction, which can result in some underestimation of the real amount of glacier changes.

5 FIELD VERIFICATION OF RESULTS

In September 2001, the author got an opportunity to participate in the hydrographic expedition to the Novaya Zemlya archipelago in the Russian Arctic and to validate the accuracy of the GINSAR technique. Preliminary measurements of the maximum velocities of several test tidewater glaciers were made in the lab using 4 ERS-1/2-INSAR models taken in March and October 1996. The frontal velocities of the same glaciers were surveyed during the field campaign using precise geodetic equipment.

The geodetic surveys were performed using two alternative techniques. A conventional geodetic technique of forward intersection is based on multitemporal observations of identical points at the glacier front from two different positions with a known baseline. The polar idea of a non-traditional "touch-and-go" technique is to install the laser line in a tangential position at a predefined distance from the glacier front and to frequently measure the distance to any point on the opposite coast in order to record the instant when the glacier will cross the laser line and the measured distance will change abruptly (Sharov et al. 2001). This technique made use of a LDI-3 laser rangefinder (range up to 19 km without retro-reflector) mounted on a Leica T1602 theodolite (angular accuracy 0.5 mgon). Schematic diagrams explaining both approaches are given in Fig. 5. Typical results of velocity measurements are given in Table 1.

Field observations have shown that, in the study region, the accuracy of (G)INSAR determinations generally decreases considerably in areas with steep slopes. The results obtained indicate that the INSAR velocities are somewhat lower than those from geodetic surveys, which corresponds to the observations performed by other investigators in other regions (e.g. Rabus & Fatland 2000). Apart from the different duration of observations and seasonal changes in the glacier motion, this fact can be explained by the inherent influence of INSAR undersampling, if the velocity gradient between two neighbouring pixels exceeds the critical value ΔV_{cr} and the width of motion fringes in the interferogram vanishes. In areas of high deformation along glacier walls and at glacier fronts with numerous crevasses and non-uniform motion of ice blocks, the motion phase gradient can exceed π, if the velocity gradient between two neighbouring pixels is larger than 0.25λ , i.e.

$$\Delta V_{cr} = V_{y+1} - V_y \geq \lambda/4 = 1.415\,[cm/day]\,. \qquad (12)$$

It was revealed that, in the test area, the daily peak of glacier activity with corresponding maximum motion rate and calving effects is attained at midday (between 11:00 and 14:00 Moscow time) and is probably related to tides. Vertical (tidal) swaying motions with an intensity of 1 – 2 cm/min have been recorded at several glaciers (Vera, Sredniy), which verifies the existence of, at least, partly floating glacier tongues in Novaya Zemlya (Sharov et al. 2001). The INSAR determinations performed at these glaciers in the lab must be redone.

In spite of the revealed tachometric differences of up to 40% and more, the spatial correlation between the GINSAR velocities and those surveyed in the field was quite high over the remaining 5 test glaciers. The next field campaign, this time to the Svartisen Ice Cap with inland glacier fronts and typically lower glacier velocities, is planned for late summer 2002.

Table 1. Glacier velocities measured in the lab and in the field

Glacier	Frontal velocity [m/day]		
	INSAR	Forward intersection	Touch-and-go
Rykatchova, No. 88	0.56	0,68±0,14	0,83±0,20
Maka, No.91	0.37	0,61±0,13	0,73±0,15

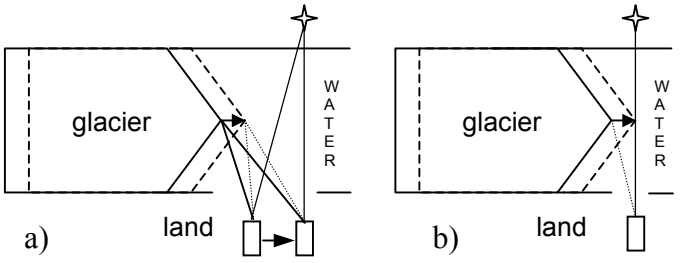

Figure 5. Schematic diagrams explaining the forward intersection (a) and "touch-and-go" (b) techniques

7 CONCLUSIONS

A new algorithm has been designed, tested and verified for INSAR modelling of glacial dynamics and morphology. Compared to the conventional DINSAR method, our algorithm based on the calculation of interferometric phase gradients, the generation of glacier slope maps and the analysis of differences between multitemporal slope maps provides simple, global and fast solutions to unsupervised glacier change detection and analysis. Apart from the technological simplicity and robustness, the GINSAR algorithm does not involve the procedure of interferometric phase unwrapping, thus excluding areal error propagation and improving the modelling accuracy. A flow chart showing the sequence of principal stages of the GINSAR algorithm is given in Fig. 6.

The GINSAR technique can be successfully applied to accounting for temporal changes in the glacier accumulation rate and the glacier mass balance at regional scale. The high metric quality, detail and complementary thematic contents of the GINSAR products, which are called *topogram, fluxogram* and *velogram,* show the expedience of this technique and its applicability to solving various tasks in the area of unsupervised change detection and analysis irrespective of INSAR data sources.

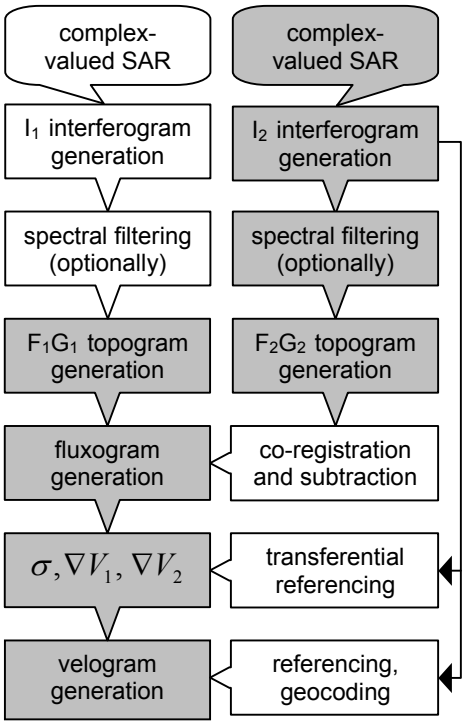

Figure 6. Principal flowchart of the GINSAR technique

Experimental studies and field surveys proved the efficacy and robustness of our new algorithm. Some 27 GINSAR models have been processed until the present time and all the results were entirely satisfactory. The time required for processing one differential model did not exceed 4 hours. The algorithm has been implemented in the new RSG 4.0 software package distributed by Joanneum Research.

ACKNOWLEDGEMENTS

The author wishes to express the warmest thanks to Prof. M. Kuhn from the Institute of Meteorology and Geophysics, Innsbruck University, for his valuable explanations on the methodology of glacier monitoring and general encouragement. Some advice on the glaciological interpretation of INSAR products were kindly provided by B.Wangenstein from the Institute of Geography, Oslo University. The experimental ERS-1/2-INSAR data set was acquired from the ESA archives in the framework of the EU OMEGA project (EESD Programme).

REFERENCES

Fatland, D., Lingle, G. 1998. Analysis of the 1993-95 Bering Glacier surge using differential SAR interferometry. *J.Glac.,* 44 (148): 532-545.

Forster, R. et al. 1999. Interferometric radar observations of Glaciares Europa and Penguin. *J.Glac.,* 45 (150) : 325-336.

Gabriel, A. et al. 1989. Mapping small elevation changes over large areas: differential radar interferometry. *J. Geophys.Res.*, 94, B7 : 9183-9191.

Kjöllmoen, B. (Ed) 2002. Glaciological investigations in Norway in 2000. The NVE report No. 2, 122 p.

Kuhn M. et al., 1999. Measurements and models of the mass balance of Hintereisferener. *Geografiska Annaler*, 81A, 4: 659-670.

Piskunov, N.S. 1978. Differential and integral calculus. V. 2, Moscow: Nauka, 575 p. (in Russian).

Rabus, B.T., Fatland, D.R. 2000. Comparison of SAR-interferometric and surveyed velocities on a mountain glacier: Black Rapids Glacier. *J.Glac.*, 46 (152): 119-128.

Sharov, A.I., Gutjahr K. 2002. Some methodological enhancements to INSAR surveying of polar ice caps. In: Observing our environment from space. Proc. of the 21st EARSeL Symp.: 65-72.

Sharov, A.I. et al. 2001. Results of the field campaign in Barents and Kara seas on board the ship "Hydrologist". In: Annual scientific report to the INCO Commission, P 9: 1-20.

Sharov, A.I. et al. 2002. Methodical alternatives to the glacier motion measurement from differential SAR interferometry. Proc. of the PCV'02 Symposium, Graz, Austria (in print).

Webster's Revised Unabridged Dictionary 1998. MICRA Inc.